# Chapter 2

# LATERAL VEHICLE DYNAMICS

The first section in this chapter provides a review of several types of lateral control systems that are currently under development by automotive manufacturers and researchers. The subsequent sections in the chapter study kinematic and dynamic models for lateral vehicle motion. Control system design for lateral vehicle applications is studied later in Chapter 3.

## 2.1 LATERAL SYSTEMS UNDER COMMERCIAL DEVELOPMENT

Lane departures are the number one cause of fatal accidents in the United States, and account for more than 39% of crash-related fatalities. Reports by the National Highway Transportation Safety Administration (NHTSA) state that as many as 1,575,000 accidents annually are caused by distracted drivers - a large percentage of which can be attributed to unintended lane departures. Lane departures are also identified by NHTSA as a major cause of rollover incidents involving sport utility vehicles (SUVs) and light trucks (http://www.nhtsa.gov).

Three types of lateral systems have been developed in the automotive industry that address lane departure accidents: lane departure warning systems (LDWS), lane keeping systems (LKS) and yaw stability control systems. A significant amount of research is also being conducted by university researchers on these types of systems.

### 2.1.1 Lane departure warning

A lane departure warning (LDW) system is a system that monitors the vehicle's position with respect to the lane and provides warning if the vehicle is about to leave the lane. An example of a commercial LDW system under development is the AutoVue LDW system by Iteris, Inc. shown in Figure 2-1.

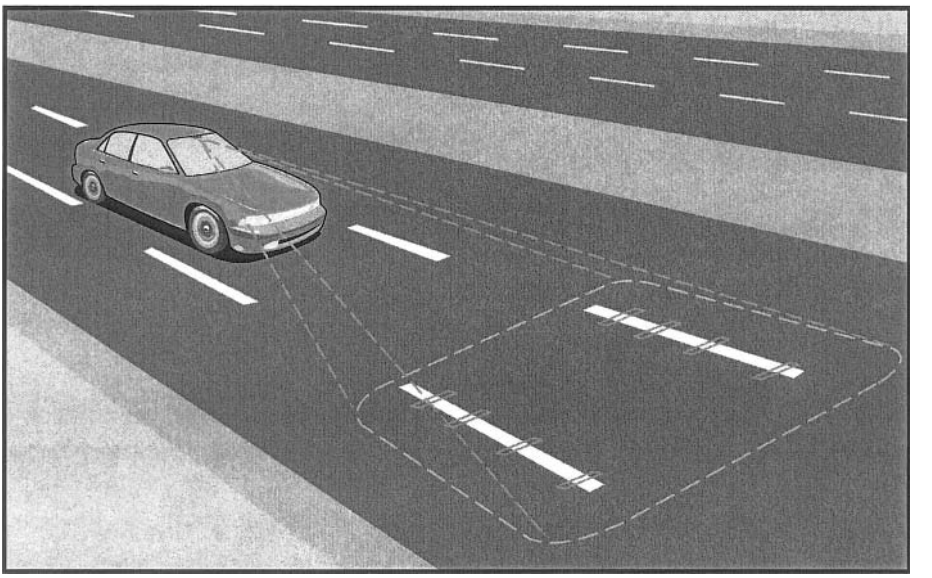

*Figure 2-1.* LDW system based on lane markings[2]

The AutoVue device is a small, integrated unit consisting of a camera, onboard computer and software that attaches to the windshield, dashboard or overhead. The system is programmed to recognize the difference between the road and lane markings. The unit's camera tracks visible lane markings and feeds the information into the unit's computer, which combines this data with the vehicle's speed. Using image recognition software and proprietary algorithms, the computer can predict when a vehicle begins to drift towards an unintended lane change. When this occurs, the unit automatically emits the commonly known rumble strip sound, alerting the driver to make a correction.

[2] Figure courtesy of Iteris, Inc.

AutoVue is publicized as working effectively both during day and night, and in most weather conditions where the lane markings are visible. By simply using the turn signal, a driver indicates to the system that a planned lane departure is intended and the alarm does not sound.

Lane departure warning systems made by Iteris are now in use on trucks manufactured by Mercedes and Freightliner. Iteris' chief competitor, *AssistWare*, has also had success in the heavy truck market: their *SafeTrac* system is now available as a factory option on *Kenworth* trucks and via direct sales to commercial fleets (http://www.assistware.com).

### 2.1.2 Lane keeping systems

A lane-keeping system automatically controls the steering to keep the vehicle in its lane and also follow the lane as it curves around. Over the last ten years, several research groups at universities have developed and demonstrated lane keeping systems. Researchers at California PATH demonstrated a lane keeping system based on the use of cylindrical magnets embedded at regular intervals in the center of the highway lane. The magnetic field from the embedded permanent magnets was used for lateral position measurement of the vehicle (Guldner, et. al., 1996). Research groups at Berkeley (Taylor, et. al., 1999) and at Carnegie Mellon (Thorpe, et. al., 1998) have developed lateral position measurement systems using vision cameras and demonstrated lateral control systems using vision based measurement. Researchers at the University of Minnesota have developed lane departure warning and lane keeping systems based on the use of differential GPS for lateral position measurements (Donath, et. al., 1997).

Systems are also under development by several automotive manufacturers, including Nissan. A lane-keeping system called LKS, which has recently been introduced in Japan on Nissan's *Cima* model, offers automatic steering in parallel with the driver (http://ivsource.net). Seeking to strike a balance between system complexity and driver responsibility, the system is targeted at 'monotonous driving' situations. The system operates only on 'straight-ish' roads (a minimum radius will eventually be specified) and above a minimum defined speed. Nissan's premise is that drivers feel tired after long hours of continuous expressway driving as a result of having to constantly steer their vehicles slightly to keep them in their lane. The LKS attempts to reduce such fatigue by improving stability on the straight highway road. But the driver must remain engaged in actively steering the vehicle -- if he/she does not, the LKS gradually reduces its degree of assistance. The practical result is that you can't "tune out" and expect the car to drive for you. Nissan's argument is that this approach achieves the difficult balance between providing driver assistance while maintaining

driver responsibility. The low level of steering force added by the control isn't enough to interfere with the driver's maneuvers.

The system uses a single CCD camera to recognize the lane demarkation, a steering actuator to steer the front wheels, and an electronic control unit. The camera estimates the road geometry and the host vehicle's position in the lane. Based on this information, along with vehicle velocity and steering wheel angle, the control unit calculates the steering torque needed to keep within the lane.

Nissan is also developing a LDW system called its Lane Departure Avoidance (LDA) system (http://ivsource.net). The LDA system aims to reduce road departure crashes by delaying a driver's deviation from the lane in addition to providing warning through audio signals and steering wheel vibrations. Nissan's LDA creates a lateral "buffer" for the driver, and kicks into action to automatically steer if the vehicle starts to depart the lane. But, unlike a true co-pilot, the system won't continue to handle the steering job -- with haptic feedback in the steering wheel, the driver is alerted to the system activation and is expected to re-assert safe control by himself or herself. The automatic steering assist is steadily reduced over a period of several seconds. So, a road departure crash is still possible, but is expected be less likely unless the driver is seriously incapacitated.

LDA is accomplished using the same basic components of LKS: a camera, a steering actuator, an electronic control unit, and a buzzer or other warning devicer.

### 2.1.3 Yaw stability control systems

Vehicle stability control systems that prevent vehicles from spinning and drifting out have been developed and recently commercialized by several automotive manufacturers. Such stability control systems are also often referred to as yaw control systems or electronic stability control systems.

Figure 2-2 schematically shows the function of a yaw control system. In this figure, the lower curve shows the trajectory that the vehicle would follow in response to a steering input from the driver if the road were dry and had a high tire-road friction coefficient. In this case the high friction coefficient is able to provide the lateral force required by the vehicle to negotiate the curved road. If the coefficient of friction were small or if the vehicle speed were too high, then the vehicle would be unable to follow the nominal motion required by the driver – it would instead travel on a trajectory of larger radius (smaller curvature), as shown in the upper curve of

Figure 2-2. The function of the yaw control system is to restore the yaw velocity of the vehicle as much as possible to the nominal motion expected by the driver. If the friction coefficient is very small, it might not be possible to entirely achieve the nominal yaw rate motion that would be achieved by the driver on a high friction coefficient road surface. In this case, the yaw control system would partially succeed by making the vehicle's yaw rate closer to the expected nominal yaw rate, as shown by the middle curve in Figure 2-2.

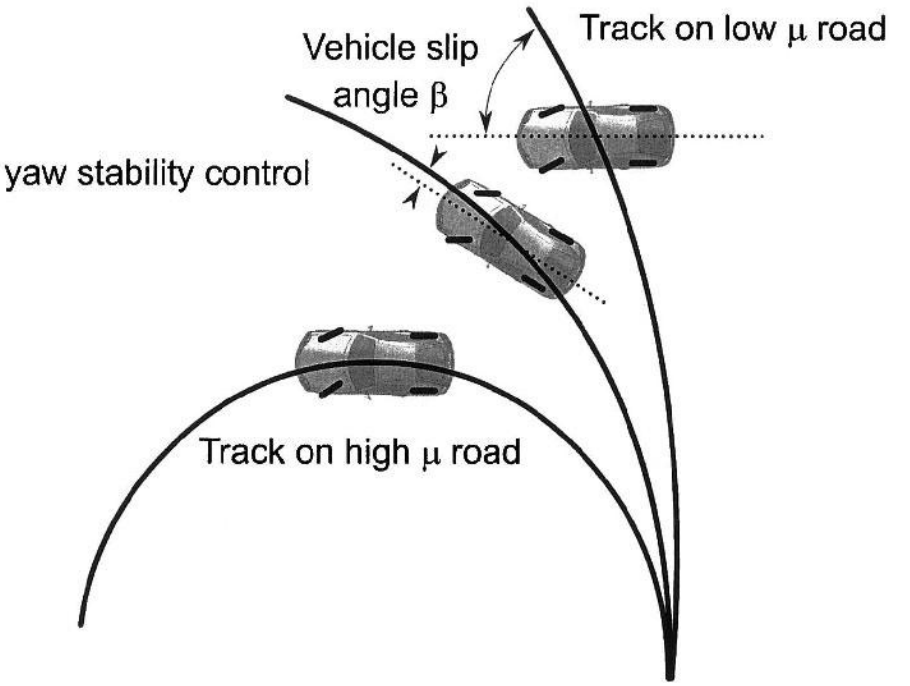


*Figure 2-2.* The functioning of a yaw control system

Many companies have investigated and developed yaw control systems during the last ten years through simulations and on prototype experimental vehicles. Some of these yaw control systems have also been commercialized on production vehicles. Examples include the BMW DSC3 (Leffler, et. al., 1998) and the Mercedes ESP, which were introduced in 1995, the Cadillac Stabilitrak system (Jost, 1996) introduced in 1996 and the Chevrolet C5 Corvette Active Handling system in 1997 (Hoffman, et.al., 1998).

Three types of stability control systems have been proposed and developed for yaw control:

**Differential Braking** systems which utilize the ABS brake system on the vehicle to apply differential braking between the right and left wheels to control yaw moment.

**Steer-by-Wire** systems which modify the driver's steering angle input and add a correction steering angle to the wheels

**Active Torque Distribution** systems which utilize active differentials and all wheel drive technology to independently control the drive torque distributed to each wheel and thus provide active control of both traction and yaw moment.

By large, the differential braking systems have received the most attention from researchers and have been implemented on several production vehicles. Steer-by-wire systems have received attention from academic researchers (Ackermann, 1994, Ackermann, 1997). Active torque distribution systems have received attention in the recent past and are likely to become available on production cars in the future.

Differential braking systems are the major focus of coverage in this book. They are discussed in section 8.2. Steer-by-wire systems are discussed in section 8.3 and active torque distribution systems are discussed in section 8.4.

## 2.2 KINEMATIC MODEL OF LATERAL VEHICLE MOTION

Under certain assumptions described below, a kinematic model for the lateral motion of a vehicle can be developed. Such a model provides a mathematical description of the vehicle motion without considering the forces that affect the motion. The equations of motion are based purely on geometric relationships governing the system.

Consider a bicycle model of the vehicle as shown in Figure 2-3 (Wang and Qi, 2001). In the bicycle model, the two left and right front wheels are represented by one single wheel at point A. Similarly the rear wheels are represented by one central rear wheel at point B. The steering angles for the front and rear wheels are represented by $\delta_f$ and $\delta_r$ respectively. The model is derived assuming both front and rear wheels can be steered. For front-wheel-only steering, the rear steering angle $\delta_r$ can be set to zero. The center of gravity (c.g.) of the vehicle is at point C. The distances of points A and B from the c.g. of the vehicle are $\ell_f$ and $\ell_r$ respectively. The wheelbase of the vehicle is $L = \ell_f + \ell_r$.

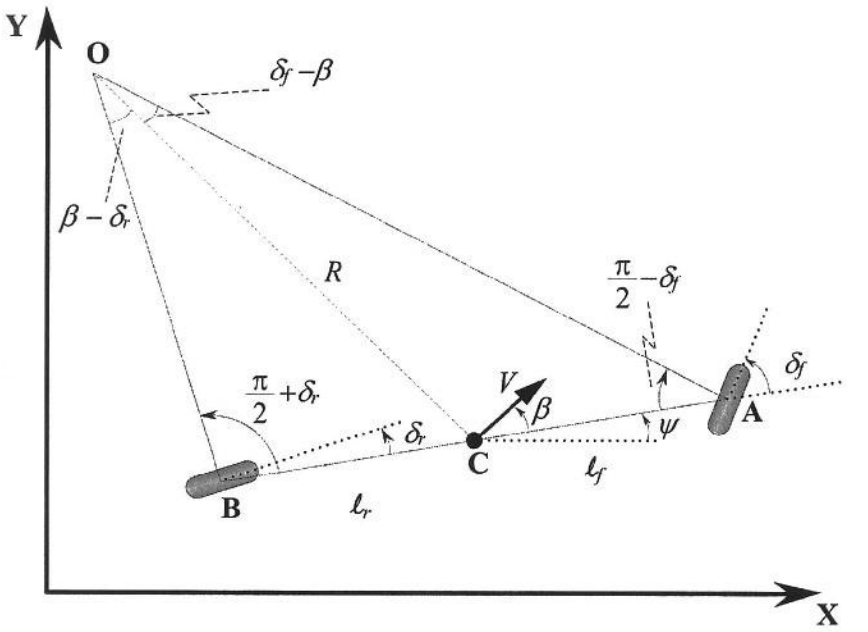


*Figure 2-3.* Kinematics of lateral vehicle motion

The vehicle is assumed to have planar motion. Three coordinates are required to describe the motion of the vehicle: $X$, $Y$ and $\psi$. $(X,Y)$ are inertial coordinates of the location of the c.g. of the vehicle while $\psi$ describes the orientation of the vehicle. The velocity at the c.g. of the vehicle is denoted by $V$ and makes an angle $\beta$ with the longitudinal axis of the vehicle. The angle $\beta$ is called the slip angle of the vehicle.

Assumptions

The major assumption used in the development of the kinematic model is that the velocity vectors at points A and B are in the direction of the orientation of the front and rear wheels respectively. In other words, the velocity vector at the front wheel makes an angle $\delta_f$ with the longitudinal axis of the vehicle. Likewise, the velocity vector at the rear wheel makes an angle $\delta_r$ with the longitudinal axis of the vehicle. This is equivalent to assuming that the "slip angles" at both wheels are zero. This is a reasonable assumption for low speed motion of the vehicle (for example, for speeds less than 5 m/s). At low speeds, the lateral force generated by the tires is small.

In order to drive on any circular road of radius $R$, the total lateral force from both tires is

$$\frac{mV^2}{R}$$

which varies quadratically with the speed $V$ and is small at low speeds. When the lateral forces are small, as explained later in section 2.4, it is indeed very reasonable to assume that the velocity vector at each wheel is in the direction of the wheel.

The point O is the instantaneous rolling center for the vehicle. The point O is defined by the intersection of lines AO and BO which are drawn perpendicular to the orientation of the two rolling wheels.

The radius of the vehicle's path $R$ is defined by the length of the line OC which connects the center of gravity C to the instantaneous rolling center O. The velocity at the c.g. is perpendicular to the line OC. The direction of the velocity at the c.g. with respect to the longitudinal axis of the vehicle is called the slip angle of the vehicle $\beta$.

The angle $\psi$ is called the heading angle of the vehicle. The course angle for the vehicle is $\gamma = \psi + \beta$.

Apply the sine rule to triangle OCA.

$$\frac{\sin(\delta_f - \beta)}{\ell_f} = \frac{\sin\left(\frac{\pi}{2} - \delta_f\right)}{R} \tag{2.1}$$

Apply the sine rule to triangle OCB.

$$\frac{\sin(\beta - \delta_r)}{\ell_r} = \frac{\sin\left(\frac{\pi}{2} + \delta_r\right)}{R} \tag{2.2}$$

From Eq. (2.1)

$$\frac{\sin(\delta_f)\cos(\beta) - \sin(\beta)\cos(\delta_f)}{\ell_f} = \frac{\cos(\delta_f)}{R} \tag{2.3}$$

From Eq. (2.2)

$$\frac{\cos(\delta_r)\sin(\beta)-\cos(\beta)\sin(\delta_r)}{\ell_r}=\frac{\cos(\delta_r)}{R} \tag{2.4}$$

Multiply both sides of Eq. (2.3) by $\frac{\ell_f}{\cos(\delta_f)}$. We get

$$\tan(\delta_f)\cos(\beta)-\sin(\beta)=\frac{\ell_f}{R} \tag{2.5}$$

Multiply both sides of Eq. (2.4) by $\frac{\ell_r}{\cos(\delta_r)}$. We get

$$\sin(\beta)-\tan(\delta_r)\cos(\beta)=\frac{\ell_r}{R} \tag{2.6}$$

Adding Eqs. (2.5) and (2.6)

$$\{\tan(\delta_f)-\tan(\delta_r)\}\cos(\beta)=\frac{\ell_f+\ell_r}{R} \tag{2.7}$$

If we assume that the radius of the vehicle path changes slowly due to low vehicle speed, then the rate of change of orientation of the vehicle (i.e. $\dot{\psi}$) must be equal to the angular velocity of the vehicle. Since the angular velocity of the vehicle is $\frac{V}{R}$, it follows that

$$\dot{\psi}=\frac{V}{R} \tag{2.8}$$

Using Eq. (2.8), Eq. (2.7) can be re-written as

$$\dot{\psi} = \frac{V\cos(\beta)}{\ell_f + \ell_r}\left(\tan(\delta_f) - \tan(\delta_r)\right) \tag{2.9}$$

The overall equations of motion are therefore given by

$$\dot{X} = V\cos(\psi + \beta) \tag{2.10}$$

$$\dot{Y} = V\sin(\psi + \beta) \tag{2.11}$$

$$\dot{\psi} = \frac{V\cos(\beta)}{\ell_f + \ell_r}\left(\tan(\delta_f) - \tan(\delta_r)\right) \tag{2.12}$$

In this model there are three inputs: $\delta_f$, $\delta_r$ and $V$. The velocity $V$ is an external variable and can be assumed to be a time varying function or can be obtained from a longitudinal vehicle model.

The slip angle $\beta$ can be obtained by multiplying Eq. (2.5) by $\ell_r$ and subtracting it from Eq. (2.6) multiplied by $\ell_f$:

$$\beta = \tan^{-1}\left(\frac{\ell_f \tan\delta_r + \ell_r \tan\delta_f}{\ell_f + \ell_r}\right) \tag{2.13}$$

**Remark**

Here it is appropriate to include a note on the "bicycle" model assumption. Both the left and right front wheels were represented by one front wheel in the bicycle model. It should be noted that the left and right steering angles in general will be approximately equal, but not exactly so. This is because the radius of the path each of these wheels travels is different. Consider a front wheel steered vehicle as shown in Figure 2-4.

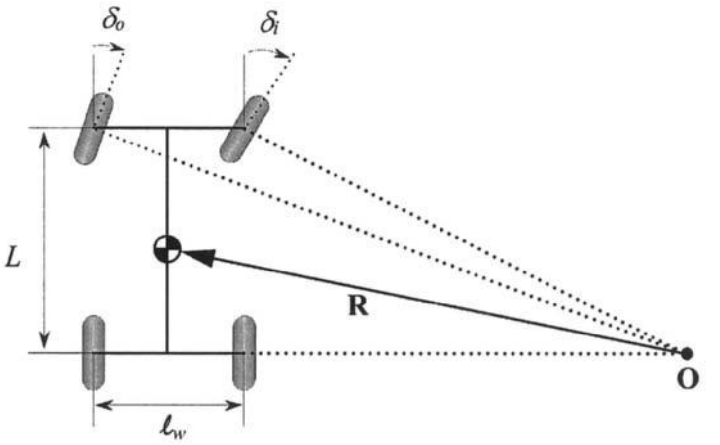


*Figure 2-4.* Ackerman turning geometry

Let $\ell_w$ be the track width of the vehicle and $\delta_o$ and $\delta_i$ be the outer and inner steering angles respectively. Let the wheelbase $L = \ell_f + \ell_r$ be small compared to the radius $R$. If the slip angle $\beta$ is small, then Eq. (2.12) can be approximated by

$$\frac{\dot{\psi}}{V} \approx \frac{1}{R} = \frac{\delta}{L}$$

or

$$\delta = \frac{L}{R} \tag{2.14}$$

Since the radius at the inner and outer wheels are different, we have

$$\delta_o = \frac{L}{R + \frac{\ell_w}{2}} \tag{2.15}$$

$$\delta_i = \frac{L}{R - \frac{\ell_w}{2}} \tag{2.16}$$

The average front wheel steering angle is approximately given by

$$\delta = \frac{\delta_o + \delta_i}{2} \cong \frac{L}{R} \tag{2.17}$$

The difference between $\delta_o$ and $\delta_i$ is

$$\delta_i - \delta_o = \frac{L}{R^2}\ell_w = \delta^2 \frac{\ell_w}{L} \tag{2.18}$$

Thus the difference in the steering angles of the two front wheels is proportional to the square of the average steering angle. Such a differential steer can be obtained from a trapezoidal tie rod arrangement, as shown in Figure 2-5. As can be seen from the figure, for both left and right turns, the inner wheel always turns a larger steering angle.

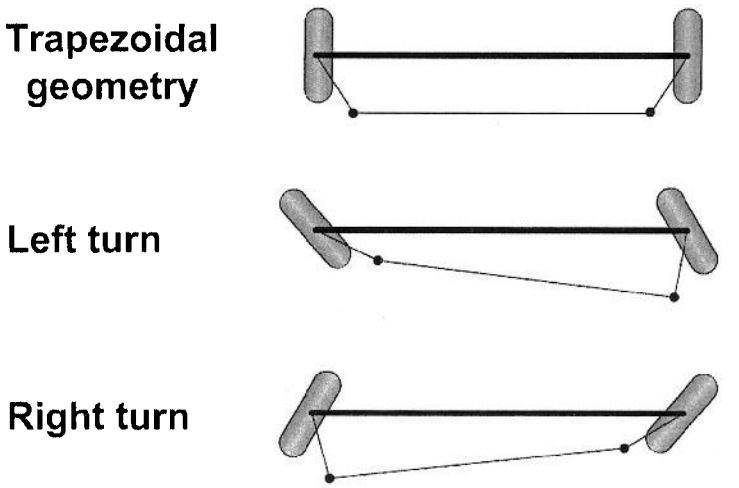


*Figure 2-5.* Differential steer from a trapezoidal tie-rod arrangement

*Table 2.1 Summary of kinematic model equations*

| SUMMARY OF KINEMATIC MODEL EQUATIONS | | |
|---|---|---|
| Symbol | Nomenclature | Equation |
| $X$ | Global $X$ axis coordinate | $\dot{X} = V\cos(\psi + \beta)$ |
| $Y$ | Global $Y$ axis coordinate | $\dot{Y} = V\sin(\psi + \beta)$ |
| $\psi$ | Yaw angle; orientation angle of vehicle with respect to global $X$ axis | $\dot{\psi} = \frac{V\cos(\beta)}{\ell_f + \ell_r}\left(\tan(\delta_f) - \tan(\delta_r)\right)$ |
| $\beta$ | Vehicle slip angle | $\beta = \tan^{-1}\left(\frac{\ell_f \tan\delta_r + \ell_r \tan\delta_f}{\ell_f + \ell_r}\right)$ |

## 2.3 BICYCLE MODEL OF LATERAL VEHICLE DYNAMICS

At higher vehicle speeds, the assumption that the velocity at each wheel is in the direction of the wheel can no longer be made. In this case, instead of a kinematic model, a dynamic model for lateral vehicle motion must be developed.

A "bicycle" model of the vehicle with two degrees of freedom is considered, as shown in Figure 2-6. The two degrees of freedom are represented by the vehicle lateral position $y$ and the vehicle yaw angle $\psi$. The vehicle lateral position is measured along the lateral axis of the vehicle to the point O which is the center of rotation of the vehicle. The vehicle yaw angle $\psi$ is measured with respect to the global $X$ axis. The longitudinal velocity of the vehicle at the c.g. is denoted by $V_x$.

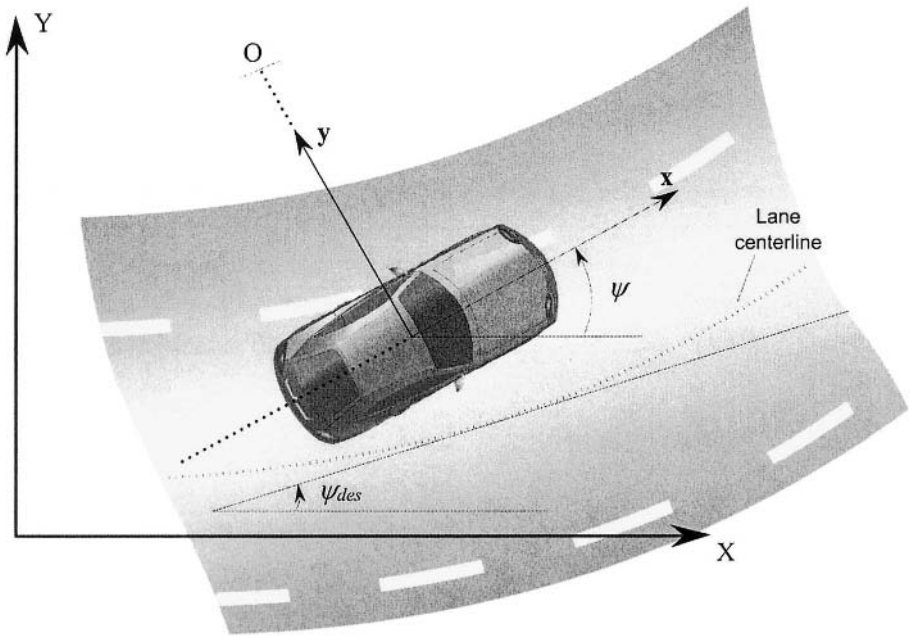


*Figure 2-6.* Lateral vehicle dynamics

The influence of road bank angle will be considered later. Ignoring road bank angle for now and applying Newton's second law for motion along the $y$ axis (Guldner, et. al., 1996),

$$ma_y = F_{yf} + F_{yr} \tag{2.19}$$

where $a_y = \left(\frac{d^2 y}{dt^2}\right)_{inertial}$ is the inertial acceleration of the vehicle at the c.g. in the direction of the $y$ axis and $F_{yf}$ and $F_{yr}$ are the lateral tire forces of the front and rear wheels respectively. Two terms contribute to $a_y$: the acceleration $\ddot{y}$ which is due to motion along the y axis and the centripetal acceleration $V_x\dot{\psi}$ . Hence

$$a_y = \ddot{y} + V_x\dot{\psi} \tag{2.20}$$

Substituting from Eq. (2.20) into Eq. (2.19), the equation for the lateral translational motion of the vehicle is obtained as

$$m(\ddot{y} + \dot{\psi}V_x) = F_{yf} + F_{yr} \tag{2.21}$$

Moment balance about the $z$ axis yields the equation for the yaw dynamics as

$$I_z\ddot{\psi} = \ell_f F_{yf} - \ell_r F_{yr} \tag{2.22}$$

where $\ell_f$ and $\ell_r$ are the distances of the front tire and the rear tire respectively from the c.g. of the vehicle.

The next step is to model the lateral tire forces $F_{yf}$ and $F_{yr}$ that act on the vehicle. Experimental results show that the lateral tire force of a tire is proportional to the "slip-angle" for small slip-angles. The slip angle of a tire is defined as the angle between the orientation of the tire and the orientation of the velocity vector of the wheel (see Figure 2-7). In Figure 2-7, the slip angle of the front wheel is

$$\alpha_f = \delta - \theta_{Vf} \tag{2.23}$$

where $\theta_{vf}$ is the angle that the velocity vector makes with the longitudinal axis of the vehicle and $\delta$ is the front wheel steering angle. The rear slip angle is similarly given by

$$\alpha_r = -\theta_{Vr} \tag{2.24}$$

A physical explanation of why the lateral tire force is proportional to slip angle can be found in Chapter 13 (in section 13.4).

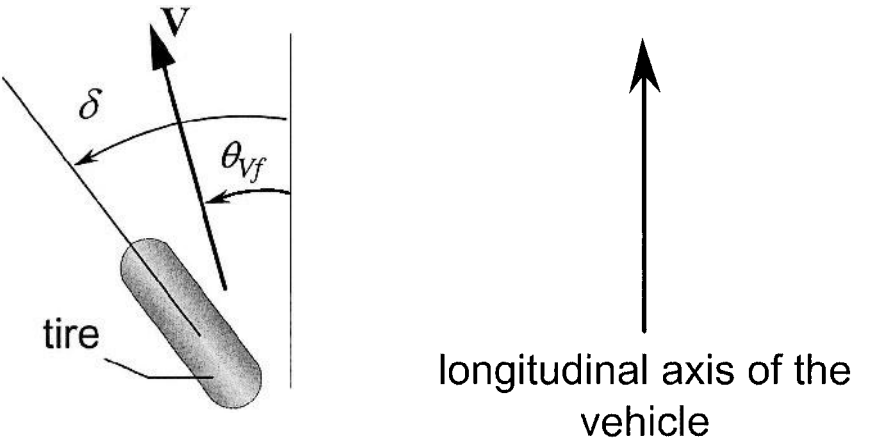


*Figure 2-7.* Tire slip-angle

The lateral tire force for the front wheels of the vehicle can therefore be written as

$$F_{yf} = 2C_{\alpha f}\left(\delta - \theta_{Vf}\right) \tag{2.25}$$

where the proportionality constant $C_{\alpha f}$ is called the cornering stiffness of each front tire, $\delta$ is the front wheel steering angle and $\theta_{Vf}$ is the front tire velocity angle. The factor 2 accounts for the fact that there are two front wheels.

Similarly the lateral tire for the rear wheels can be written as

$$F_{yr} = 2C_{\alpha r}\left(-\theta_{Vr}\right) \tag{2.26}$$

where $C_{\alpha r}$ is the cornering stiffness of each rear tire and $\theta_{V\,r}$ is the rear tire velocity angle.

The following relations can be used to calculate $\theta_{Vf}$ and $\theta_{V\,r}$:

$$\tan(\theta_{Vf}) = \frac{V_y + \ell_f \dot{\psi}}{V_x} \tag{2.27}$$

$$\tan(\theta_{Vr}) = \frac{V_y - \ell_r \dot{\psi}}{V_x} \tag{2.28}$$

Using small angle approximations and using the notation $V_y = \dot{y}$,

$$\theta_{Vf} = \frac{\dot{y} + \ell_f \dot{\psi}}{V_x} \tag{2.29}$$

$$\theta_{Vr} = \frac{\dot{y} - \ell_r \dot{\psi}}{V_x} \tag{2.30}$$

Substituting from Eqs. (2.23), (2.24), (2.29) and (2.30) into Eqs. (2.21) and (2.22), the state space model can be written as

$$\frac{d}{dt}\begin{Bmatrix} y \\ \dot{y} \\ \psi \\ \dot{\psi} \end{Bmatrix} = \begin{bmatrix} 0 & 1 & 0 & 0 \\ 0 & -\dfrac{2C_{\alpha f} + 2C_{\alpha r}}{mV_x} & 0 & -V_x - \dfrac{2C_{\alpha f}\ell_f - 2C_{\alpha r}\ell_r}{mV_x} \\ 0 & 0 & 0 & 1 \\ 0 & -\dfrac{2\ell_f C_{\alpha f} - 2\ell_r C_{\alpha r}}{I_z V_x} & 0 & -\dfrac{2\ell_f{}^2 C_{\alpha f} + 2\ell_r{}^2 C_{\alpha r}}{I_z V_x} \end{bmatrix} + \begin{Bmatrix} 0 \\ \dfrac{2C_{\alpha f}}{m} \\ 0 \\ \dfrac{2\ell_f C_{\alpha f}}{I_z} \end{Bmatrix} \delta \tag{2.31}$$

**Consideration of road bank angle**

If the influence of road bank angles is included, then Eq. (2.21) can be rewritten as

$$m(\ddot{y} + \dot{\psi} V_x) = F_{yf} + F_{yr} + F_{bank} \tag{2.32}$$

where $F_{bank} = mg\sin(\phi)$ and $\phi$ is the road bank angle with sign convention as shown in Figure 2-8.

The yaw dynamics of the vehicle are not affected by road bank angle. Hence Eq. (2.22) remains the same even in the presence of a bank angle.

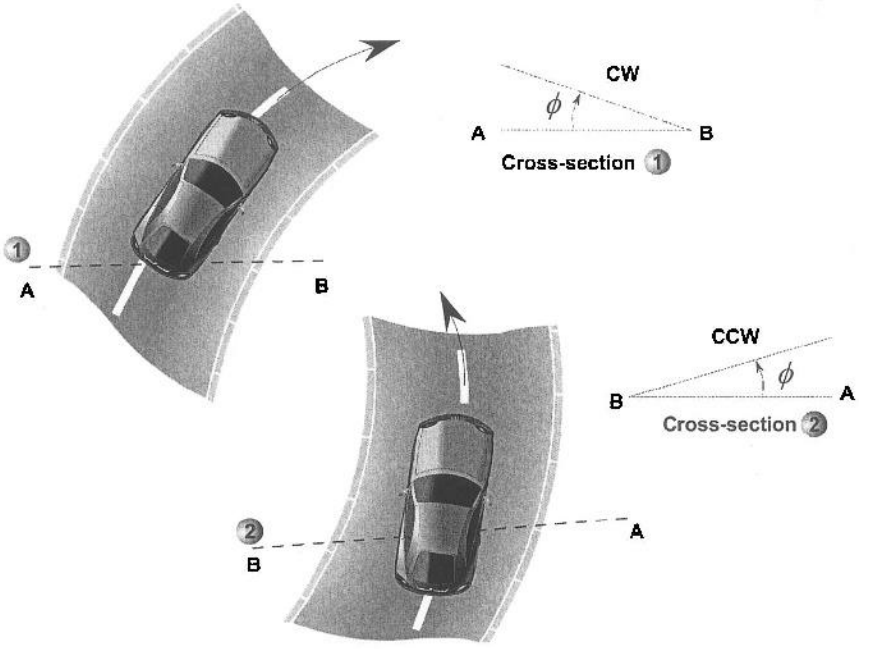


*Figure 2-8.* Sign convention for bank angle

**Comment on lateral tire forces at larger slip angles**

The assumption that the lateral tire force is proportional to slip angle will not hold at large slip angles. In such cases, the lateral tire force will depend on slip angle, the normal tire load $F_z$, the tire-road friction coefficient $\mu$ and also the magnitude of longitudinal tire force that is being simultaneously generated. For a more complete lateral tire model that includes the

influence of all these variables, see chapter 13 of this book. At large slip angles, the tire model will no longer be linear.

## 2.4 MOTION OF A PARTICLE RELATIVE TO A ROTATING FRAME

This section describes the relation between acceleration in body fixed coordinates and acceleration in inertial coordinates for a general rotating rigid body. This formulation can be used to obtain inertial acceleration values of a vehicle with yaw rate, roll and pitch rotational motion. In this section, the formulation is used to obtain inertial acceleration along the lateral axis of a vehicle which has rotational yaw motion.

Consider a rotating body, as shown in Figure 2-9, described in two coordinate systems : a coordinate system fixed in inertial space (XYZ) and a coordinate system fixed to the body (xyz). At the time instant under consideration, assume that both coordinate systems have the same orientation. Let the angular speed of the body be $\vec{\Omega}$.

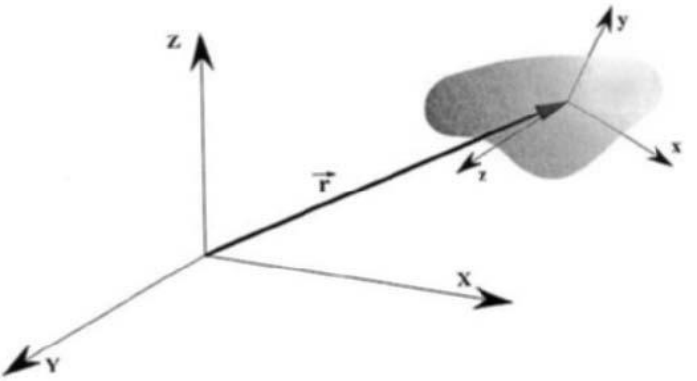


*Figure 2-9.* Inertial and body-fixed coordinate systems

Consider a particle P with inertial coordinates $[X \quad Y \quad Z]^T$ and body-fixed coordinates $[x \quad y \quad z]^T$ located on the body. Let $\vec{r}$ be the vector from the origin of the inertial coordinate system to the point P. The

acceleration of this particle in inertial coordinates can be related to its acceleration in body-fixed coordinates as follows (Merriam and Kraige, 1987):

$$\frac{d^2}{dt^2}\begin{Bmatrix} X \\ Y \\ Z \end{Bmatrix} = \frac{d^2}{dt^2}\begin{Bmatrix} x \\ y \\ z \end{Bmatrix} + \vec{\Omega} \text{ x } (\vec{\Omega} \text{ x } \vec{r}) + \dot{\vec{\Omega}} \text{ x } \vec{r} + 2\,\vec{\Omega} \text{ x } \dot{\vec{r}} \qquad (2.33)$$

All the vectors on the right-hand side of the above equation are expressed in body-fixed coordinates.

Apply Eq. (2.33) to the case of the lateral vehicle system shown in Figure 2-10.

Let $\hat{i}, \hat{j}, \hat{k}$ be unit vectors in the direction of the $x, y, z$ axes. We have

$$\vec{\Omega} = \dot{\psi}\,\hat{k} \qquad (2.34)$$

$$\vec{r} = -R\hat{j} \qquad (2.35)$$

From Eq. (2.33)

$$\vec{a}_{inertial} = \vec{\Omega} \text{ x } (\vec{\Omega} \text{ x } \vec{r}) + \dot{\vec{\Omega}} \text{ x } \vec{r} + 2\,\vec{\Omega} \text{ x } \dot{\vec{r}} + \vec{a}_{body\_fixed}$$

or

$$\vec{a}_{inertial} = \dot{\psi}\hat{k} \text{ x } (\dot{\psi}\hat{k} \text{ x } -\text{R}\hat{\text{j}}) + \ddot{\psi}\,\hat{k} \text{ x } -\text{R}\hat{\text{j}} + 2\,\dot{\psi}\,\hat{k} \text{ x } -\dot{\text{R}}\hat{j} + \ddot{x}\,\hat{i} + \ddot{y}\,\hat{j}$$

or

$$\vec{a}_{inertial} = \dot{\psi}^2 R\,\hat{j} + (R\ddot{\psi} + 2\dot{\psi}\dot{R})\,\hat{i} + \ddot{x}\,\hat{i} + \ddot{y}\,\hat{j} \qquad (2.36)$$

Hence $a_y = \dot{\psi}^2 R + \ddot{y} = V_x\dot{\psi} + \ddot{y}$.

Hence the inertial acceleration along the $y$ axis is

$$a_y = \ddot{y} + V_x \dot{\psi} \tag{2.37}$$

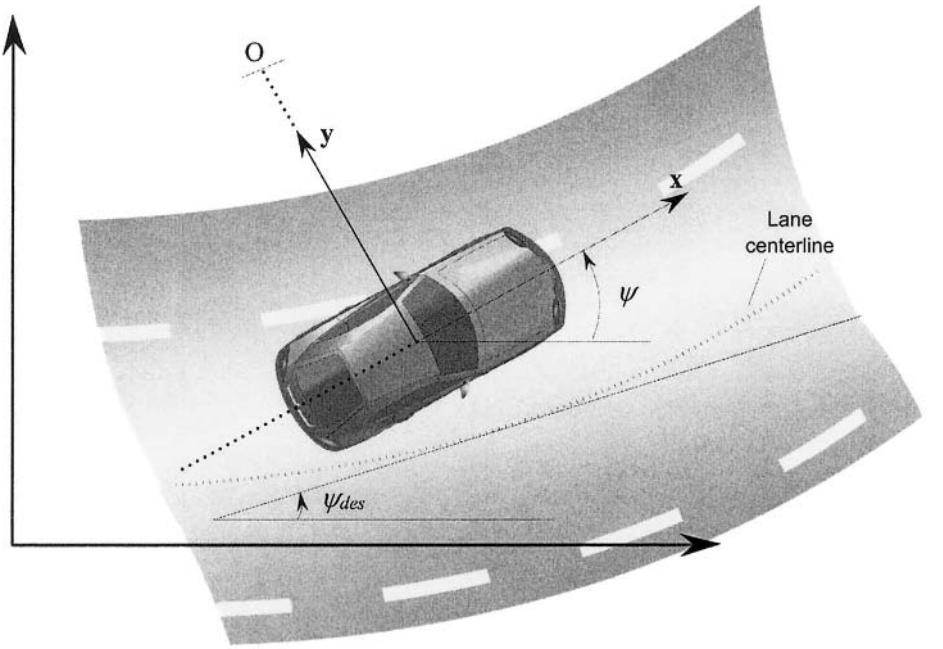


*Figure 2-10.* The lateral system in terms of rotating coordinates

## 2.5 DYNAMIC MODEL IN TERMS OF ERROR WITH RESPECT TO ROAD

When the objective is to develop a steering control system for automatic lane keeping, it is useful to utilize a dynamic model in which the state variables are in terms of position and orientation error with respect to the road.

Hence the lateral model developed in section 2.3 will be re-defined in terms of the following error variables:

$e_1$, the distance of the c.g. of the vehicle from the center line of the lane

$e_2$, the orientation error of the vehicle with respect to the road.

Consider a vehicle traveling with constant longitudinal velocity $V_x$ on a road of constant radius $R$. Again, assume that the radius $R$ is large so that

the same small angle assumptions as in the previous section can be made. Define the rate of change of the desired orientation of the vehicle as

$$\dot{\psi}_{des} = \frac{V_x}{R} \tag{2.38}$$

The desired acceleration of the vehicle can then be written as

$$\frac{V_x^{\,2}}{R} = V_x \dot{\psi}_{des} \tag{2.39}$$

Define $\ddot{e}_1$ and $e_2$ as follows (Guldner, et. al., 1996):

$$\ddot{e}_1 = (\ddot{y} + V_x \dot{\psi}) - \frac{V_x^{\,2}}{R} = \ddot{y} + V_x(\dot{\psi} - \dot{\psi}_{des}) \tag{2.40}$$

and

$$e_2 = \psi - \psi_{des} \tag{2.41}$$

Define

$$\dot{e}_1 = \dot{y} + V_x(\psi - \psi_{des}) \tag{2.42}$$

Eq. (2.42) is consistent with Eq. (2.40) if the velocity $V_x$ is constant. If the velocity were not constant, one would integrate Eq. (2.40) and obtain

$$\dot{e}_1 = \dot{y} + \int V_x e_2 dt$$

This would yield a model that is nonlinear and time varying and would not be useful for control system design. Hence the approach taken is to assume the longitudinal velocity is constant and obtain a LTI model. If the velocity varies, the LTI model is replaced with an LPV model in which longitudinal velocity is a time varying parameter (see section 3.4 in the next chapter).

Substituting from Eqs. (2.41) and (2.42) into (2.21) and (2.22), we find

$$
\begin{aligned}
m\ddot{e}_1 = \dot{e}_1\left[-\frac{2}{V_x}C_{\alpha f} - \frac{2}{V_x}C_{\alpha r}\right] + e_2\left[2C_{\alpha f} + 2C_{\alpha r}\right] \\
+ \dot{e}_2\left[-\frac{2C_{\alpha f}\ell_f}{V_x} + \frac{2C_{\alpha r}\ell_r}{V_x}\right] \\
+ \dot{\psi}_{des}\left[-\frac{2C_{\alpha f}\ell_f}{V_x} + \frac{2C_{\alpha r}\ell_r}{V_x}\right] + 2C_{\alpha f}\delta
\end{aligned}
\tag{2.43}
$$

and

$$
\begin{aligned}
I_z\ddot{e}_2 = 2C_{\alpha f}\ell_1\delta + \dot{e}_1\left[-\frac{2C_{\alpha f}\ell_f}{V_x} + \frac{2C_{\alpha r}\ell_r}{V_x}\right] \\
+ e_2\left[2C_{\alpha f}\ell_f - 2C_{\alpha r}\ell_r\right] + \dot{e}_2\left[-\frac{2C_{\alpha f}\ell_f{}^2}{V_x} - \frac{2C_{\alpha r}\ell_r{}^2}{V_x}\right] \\
- I_z\ddot{\psi}_{des} + \dot{\psi}_{des}\left[-\frac{2C_{\alpha f}\ell_f{}^2}{V_x} - \frac{2C_{\alpha r}\ell_r{}^2}{V_x}\right]
\end{aligned}
\tag{2.44}
$$

The state space model in tracking error variables is therefore given by

$$
\frac{d}{dt}\begin{bmatrix} e_1 \\ \dot{e}_1 \\ e_2 \\ \dot{e}_2 \end{bmatrix} =
$$

$$\begin{bmatrix} 0 & 1 & 0 & 0 \\ 0 & -\dfrac{2C_{\alpha f}+2C_{\alpha r}}{mV_x} & \dfrac{2C_{\alpha f}+2C_{\alpha r}}{m} & \dfrac{-2C_{\alpha f}\ell_f+2C_{\alpha r}\ell_r}{mV_x} \\ 0 & 0 & 0 & 1 \\ 0 & -\dfrac{2C_{\alpha f}\ell_f-2C_{\alpha r}\ell_r}{I_zV_x} & \dfrac{2C_{\alpha f}\ell_f-2C_{\alpha r}\ell_r}{I_z} & -\dfrac{2C_{\alpha f}\ell_f^2+2C_{\alpha r}\ell_r^2}{I_zV_x} \end{bmatrix} \begin{bmatrix} e_1 \\ \dot{e}_1 \\ e_2 \\ \dot{e}_2 \end{bmatrix}$$

$$+\begin{bmatrix} 0 \\ \dfrac{2C_{\alpha f}}{m} \\ 0 \\ \dfrac{2C_{\alpha f}\ell_f}{I_z} \end{bmatrix}\delta+\begin{bmatrix} 0 \\ -\dfrac{2C_{\alpha f}\ell_f-2C_{\alpha r}\ell_r}{mV_x}-V_x \\ 0 \\ -\dfrac{2C_{\alpha f}\ell_f^2+2C_{\alpha r}\ell_r^2}{I_zV_x} \end{bmatrix}\dot{\psi}_{des} \tag{2.45}$$

The tracking objective of the steering control problem can therefore be expressed as a problem of stabilizing the dynamics given by Eq. (2.45). Note that the lateral dynamics model shown above is a function of the longitudinal vehicle speed $V_x$ which has been assumed to be constant.

If the influence of road bank angle is included, then Eq. (2.45) gets rewritten as

$$\frac{d}{dt}\begin{bmatrix} e_1 \\ \dot{e}_1 \\ e_2 \\ \dot{e}_2 \end{bmatrix}=\begin{bmatrix} 0 \\ \dfrac{2C_{\alpha f}}{m} \\ 0 \\ \dfrac{2C_{\alpha f}\ell_f}{I_z} \end{bmatrix}\delta+\begin{bmatrix} 0 \\ -\dfrac{2C_{\alpha f}\ell_f-2C_{\alpha r}\ell_r}{mV_x}-V_x \\ 0 \\ -\dfrac{2C_{\alpha f}\ell_f^2+2C_{\alpha r}\ell_r^2}{I_zV_x} \end{bmatrix}\dot{\psi}_{des}+\begin{bmatrix} 0 \\ g \\ 0 \\ 0 \end{bmatrix}\sin(\phi)$$

$$+\begin{bmatrix} 0 & 1 & 0 & 0 \\ 0 & -\dfrac{2C_{\alpha f}+2C_{\alpha r}}{mV_x} & \dfrac{2C_{\alpha f}+2C_{\alpha r}}{m} & \dfrac{-2C_{\alpha f}\ell_f+2C_{\alpha r}\ell_r}{mV_x} \\ 0 & 0 & 0 & 1 \\ 0 & -\dfrac{2C_{\alpha f}\ell_f-2C_{\alpha r}\ell_r}{I_zV_x} & \dfrac{2C_{\alpha f}\ell_f-2C_{\alpha r}\ell_r}{I_z} & -\dfrac{2C_{\alpha f}\ell_f^2+2C_{\alpha r}\ell_r^2}{I_zV_x} \end{bmatrix} \begin{bmatrix} e_1 \\ \dot{e}_1 \\ e_2 \\ \dot{e}_2 \end{bmatrix}$$

(2.46)

*Table 2.2 Summary of dynamic model equations in terms of error with respect to road*

| SUMMARY OF DYNAMIC MODEL EQUATIONS | | |
|---|---|---|
| Symbol | Nomenclature | Equation |
| $x$ | State space vector | $x = [e_1 \quad \dot{e}_1 \quad e_2 \quad \dot{e}_2]^T$ |
| | | $\dot{x} = Ax + B_1\delta + B_2\dot{\psi}_{des} + B_3\sin(\phi)$ |
| | | Matrices $A$, $B_1$, $B_2$ and $B_3$ are defined in equation (2.46) |
| $e_1$ | Lateral position error with respect to road | $\ddot{e}_1 = \ddot{y} + V_x(\dot{\psi} - \dot{\psi}_{des})$ |
| $e_2$ | Yaw angle error with respect to road | $e_2 = (\psi - \psi_{des})$ |
| $\delta$ | Front wheel steering angle | |
| $\dot{\psi}_{des}$ | Desired yaw rate determined from road radius $R$ | $\dot{\psi}_{des} = \frac{V_x}{R}$ |
| $\phi$ | Bank angle with sign convention as defined by Fig. 2.9 | |

## 2.6 DYNAMIC MODEL IN TERMS OF YAW RATE AND SLIP ANGLE

In Figure 2-11, vehicle sideslip angle $\beta$ is defined as the angle between the longitudinal axis of the vehicle and the orientation of vehicle velocity

vector, and $r \equiv \dot{\psi}$ is the yaw rate of the vehicle body. The lateral dynamics of the vehicle is controlled by the front wheel steering angle $\delta$.

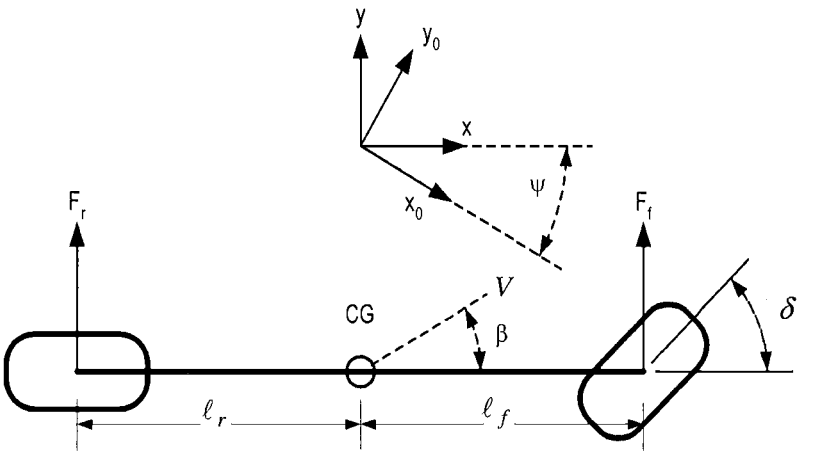


*Figure 2-11.* Single track model for vehicle lateral dynamics

The body side slip angle can be related to $e_1$ and $e_2$ as follows. Under small angle assumptions

$$\beta = \frac{\dot{y}}{V_x} = \frac{1}{V_x}(\dot{e}_1 - V_x e_2) = \frac{1}{V_x}\dot{e}_1 - e_2 \tag{2.47}$$

Using the body side slip angle $\beta$ and the yaw rate of vehicle body $r \equiv \dot{\psi}$ as state variables, the vehicle lateral dynamics can then be described by the following differential equations (Ackerman, 1997):

$$mV_x\left(\frac{d\beta}{dt} + \dot{\psi}\right) = mV_x\left(\frac{d\beta}{dt} + r\right) = F_{yf} + F_{yr} + F_{bank} \tag{2.48}$$

$$I_z\ddot{\psi} = I_z\dot{r} = \ell_f F_{yf} - \ell_r F_{yr} \tag{2.49}$$

where $m$ is vehicle mass, $V_x$ is vehicle longitudinal velocity, $F_{yf}$, $F_{yr}$ are front and rear tire forces, respectively, $F_{bank}$ is the force due to road bank

angle, $I_z$ is yaw moment of inertia, and $\ell_f$, $\ell_r$ are distances from CG (center of gravity) to front and rear tires, respectively.

For small tire slip angles, the lateral tire forces can be approximated as a linear function of tire slip angle. The front and rear tire forces and tire slip angles are defined as follows:

$$F_{yf} = C_{\alpha f}\alpha_f,\ \alpha_f = \delta - \theta_{vf} = \delta - \beta - \frac{\ell_f r}{V_x} \tag{2.50}$$

$$F_{yr} = C_{\alpha r}\alpha_r,\ \alpha_r = -\theta_{vr} = -\beta + \frac{\ell_r r}{V_x} \tag{2.51}$$

where $C_{\alpha f}$ and $C_{\alpha r}$ are the cornering stiffness of the front and rear tires respectively. Substituting (2.50) and (2.51) into (2.48) and (2.49) yields the following description for the vehicle lateral dynamics:

$$\frac{d\beta}{dt} = -r + \frac{C_{\alpha f}}{mV_x}\left(\delta - \beta - \frac{\ell_f r}{V_x}\right) + \frac{C_{\alpha r}}{mV_x}\left(-\beta + \frac{\ell_r r}{V_x}\right) + \frac{g\sin\phi}{V_x} \tag{2.52}$$

$$\frac{dr}{dt} = \frac{\ell_f C_{\alpha f}}{I_z}\left(\delta - \beta - \frac{\ell_f r}{V_x}\right) - \frac{\ell_r C_{\alpha r}}{I_z}\left(-\beta + \frac{\ell_r r}{V_x}\right) \tag{2.53}$$

## 2.7 FROM BODY FIXED TO GLOBAL COORDINATES

The dynamic model described in sections 2.5 is based on body fixed coordinates. It is suitable for control system design, since a lane keeping controller must utilize body fixed measurements of position error with respect to road. To obtain a global picture of the trajectory traversed by the vehicle, however, the time history of the body-fixed coordinates must be converted into trajectories in inertial space.

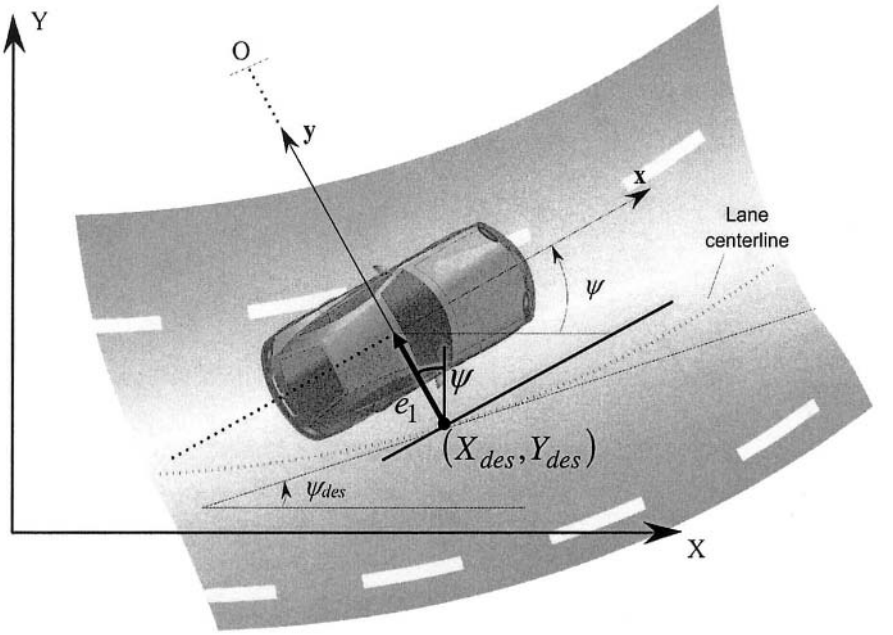


*Figure 2-12.* From body fixed to global coordinates

As shown in Figure 2-12, the lateral distance between the c.g. of the vehicle and the road centerline is $e_1$. The position of the vehicle in global coordinates is therefore given by

$$X = X_{des} - e_1 \sin(\psi) \tag{2.54}$$

$$Y = Y_{des} + e_1 \cos(\psi) \tag{2.55}$$

where $(X_{des}, Y_{des})$ are the global coordinates of the point on the road centerline which lies on a line along the lateral axis of the vehicle.

Using $X_{des} = \int_0^t V\cos(\psi_{des})dt$, $Y_{des} = \int_0^t V\sin(\psi_{des})dt$ and replacing $\psi$ by $\psi = e_2 + \psi_{des}$ in equations (2.54) and (2.55), the global coordinates of the vehicle are obtained as

$$X = \int_0^t V\cos(\psi_{des})dt - e_1\sin(e_2 + \psi_{des}) \tag{2.56}$$

$$Y = \int_0^t V\sin(\psi_{des})dt + e_1\cos(e_2 + \psi_{des}) \tag{2.57}$$

## 2.8 ROAD MODEL

The curvature of a road is the inverse of the road radius i.e. $\frac{1}{R}$. Continuity of curvature is an important criterion that a road should satisfy in order to ensure that the lateral control system can track it. Clothoid spirals are curves that are used to transition smoothly from one curvature value to another (for example, in going from a straight road to a circular road).

A clothoid is defined to be a spiral whose curvature is a linear function of its arc length and is mathematically defined in terms of Fresnel integrals (Kiencke and Nielsen, 2000). The parametric equation of a clothoid is

$$\begin{bmatrix} x(t) \\ y(t) \end{bmatrix} = a\begin{bmatrix} C(t) \\ S(t) \end{bmatrix} \tag{2.58}$$

where the scaling factor $a$ is positive, the parameter $t$ is non-negative, and the Fresnel integrals are represented as

$$C(t) = \int_0^t \cos\left(\frac{\pi u^2}{2}\right) du \tag{2.59}$$

$$S(t) = \int_0^t \sin\left(\frac{\pi u^2}{2}\right) du \tag{2.60}$$

The clothoid in Eq. (2.58) (in its standard form) is in the first quadrant and starts at $t = 0$ and converges to $\left(\frac{a}{2}, \frac{a}{2}\right)$ as $t \to \infty$. Figure 2-13 shows a clothoid spiral using $a = 6000$.

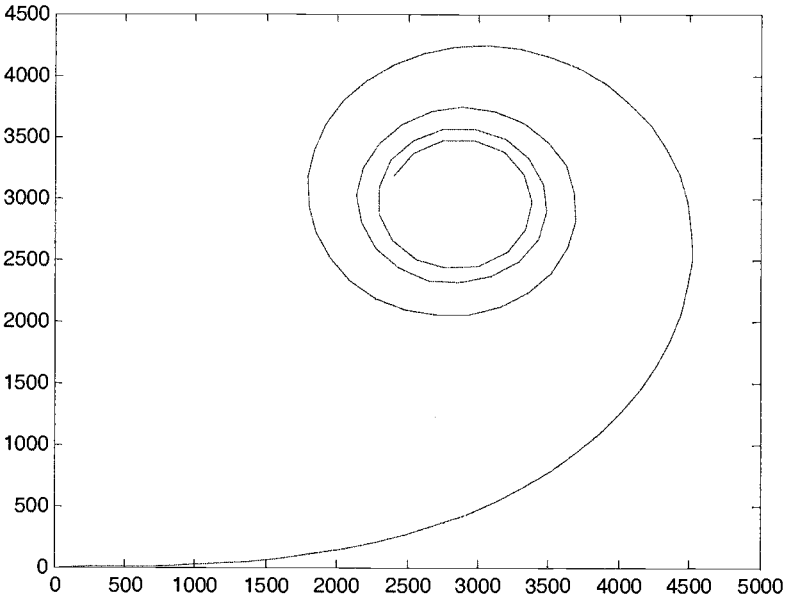


*Figure 2-13.* Clothoid spiral using a scaling value a= 6000

The integrals of the Fresnel integrals are

$$C_I(t) = \int_0^t C(u)du = tC(t) - \frac{1}{\pi}\sin\left(\frac{\pi t^2}{2}\right) \tag{2.61}$$

$$S_I(t) = \int_0^t S(u)du = tS(t) + \frac{1}{\pi}\cos\left(\frac{\pi t^2}{2}\right) - \frac{1}{\pi} \tag{2.62}$$

The following geometric formulae for clothoids shown in Table 2.3 are often useful for designing clothoids to transition from a straight line to a circle or from one circle to a circle of different radius (Sasipalli, et. al., 1997).

*Table 2.3 Geometric Formulae of Clothoids*

| Geometric Formulae of Clothoids | | |
|---|---|---|
| | Geometric Element | Parametric Expression |
| 1 | angle of tangent | $\frac{\pi}{2}t^2$ |
| 2 | curvature | $\frac{\pi}{a}t$ |
| 3 | arc length | $ds = a\,dt$ |
| 4 | center of circle of curvature | $\left(\frac{a}{t}C_I(t), \frac{a}{t}\left\{S_I(t) + \frac{1}{\pi}\right\}\right)$ |

Calculation of the cartesian coordinates from Eqs. (2.59) and (2.60) has to be done numerically i.e. the above integrals cannot be evaluated

analytically. Figure 2-14 shows a clothoid spiral used to transition from a straight line segment to a circular arc.

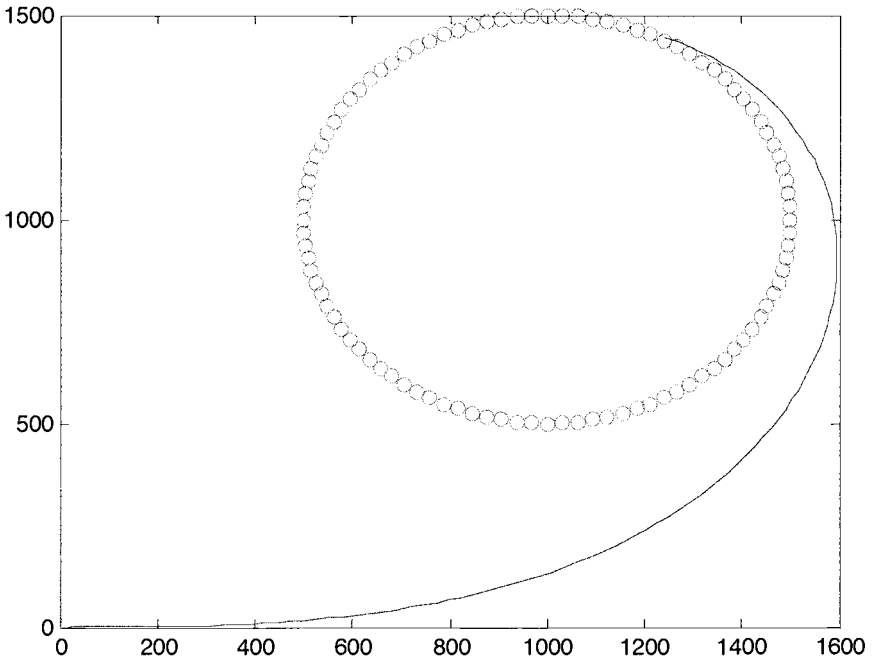


*Figure 2-14.* Clothoid spiral joining a straight line and a circle.

## 2.9 CHAPTER SUMMARY

This chapter discussed a variety of models that describe lateral vehicle motion. These models can be used to design steering control systems for lateral lane keeping. These models can also be extended for use in yaw stability control, rollover control and other vehicle control applications.

The major lateral models discussed in the chapter were

1. Kinematic vehicle model
2. Dynamic vehicle model in terms of inertial lateral position and yaw angle
3. Dynamic vehicle model in terms of road-error variables
4. Dynamic vehicle model in terms of yaw rate and vehicle slip angle

The kinematic model provides equations of motion purely in terms of geometric relationships governing the system. It is a useful model for very low speed applications, for example vehicle control for automated parking.

The dynamic models discussed in this chapter are useful for lane keeping applications and can also be extended for use in yaw stability control and rollover prevention applications. The extension and use of these models for yaw stability control is discussed in Chapter 8.

The transformation of coordinates from body-fixed to global axes was also presented. In addition road models were discussed and the use of clothoid spirals to transition smoothly from one road curvature to another was described.

## NOMENCLATURE

| | |
|---|---|
| $F_y$ | lateral tire force |
| $F_{yf}$ | lateral tire force on front tires |
| $F_{yr}$ | lateral tire force on rear tires |
| $V_x$ | longitudinal velocity at c.g. of vehicle |
| $V$ | total velocity at c.g. of vehicle |
| $\dot{y}$ | lateral velocity at c.g. of vehicle |
| $V_y$ | lateral velocity at c.g. of vehicle (same as $\dot{y}$) |
| $m$ | total mass of vehicle |
| $I_z$ | yaw moment of inertia of vehicle |
| $\ell_f$ | longitudinal distance from c.g. to front tires |
| $\ell_r$ | longitudinal distance from c.g. to rear tires |
| $L$ | total wheel base ($\ell_f + \ell_r$) |
| $\psi$ | yaw angle of vehicle in global axes |
| $\dot{\psi}$ | yaw rate of vehicle |
| $r$ | yaw rate of vehicle (same as $\dot{\psi}$) |
| $X$ , $Y$ | global axes |
| $\delta$ | steering wheel angle |

| | |
|---|---|
| $\delta_f$ | front wheel steering angle |
| $\delta_r$ | rear wheel steering angle |
| $\delta_o$ | steering angle of outer wheels |
| $\delta_i$ | steering angle of inner wheels |
| $\ell_w$ | track width |
| $\alpha_f$ | slip angle at front tires |
| $\alpha_r$ | slip angle at rear tires |
| $C_\alpha$ | cornering stiffness of tire |
| $F_z$ | normal force on tire |
| $\mu$ | tire-road friction coefficient |
| $\dot{\psi}_{des}$ | desired yaw rate from road |
| $\beta$ | slip angle at vehicle c.g. (center of gravity) |
| $\theta_V$ | velocity angle (angle of velocity vector with longitudinal axis) |
| $\phi$ | road bank angle |
| $R$ | turn radius of vehicle or radius of road |
| $e_1$ | lateral position error with respect to road |
| $e_2$ | yaw angle error with respect to road |
| $C(t)$ | Fresnel integral |
| $S(t)$ | Fresnel integral |

## REFERENCES

Ackerman, J., "Robust control prevent car skidding, " *IEEE Control Systems Magazine*, Vol. 17, No. 3, June 1997, pp. 23-31.

Donath, M., Morellas, V., Morris, T. and Alexander, L., "Preview based control of a tractor trailer using DGPS for preventing road departure accidents", *Proceedings of the IEEE Conference on Intelligent Transportation Systems*, ITSC'97, Boston, MA, November, 1997.

Guldner, J., Tan, H.-S. and Patwardhan, S., "Analysis of automatic steering control for highway vehicle with look-down lateral reference systems", *Vehicle System Dynamics,* vol. 26, no. 4, pp.243-269, 1996.

Hoffman, D. and Rizzo, M., "Chevrolet C5 Corvette vehicle dynamic control system," *SAE Technical Paper Series,* SAE-980233, 1998.

Jost, K., "Cadillac stability enhancement," *Automotive Engineering,* October, 1996.

Kiencke, U. and Nielsen, L., *Automotive Control Systems for Engine, Driveline and Vehicle*, SAE International, ISBN 0-7680-0505-1, 2000.

Leffler, H., Auffhammer, R., Heyken, R. and Roth, H., "New driving stability control system with reduced technical effort for compact and medium class passenger cars," *SAE Technical Paper Series,* SAE-980234, 1998.

Meriam, J.L. and Kraige, L.G., "Engineering Mechanics: Dynamics", Fifth Edition, John Wiley & Sons, Inc., New York, ISBN 047126606X, 2003.

Peng, H. and Tomizuka, M., "Preview control for vehicle lateral guidance in highway automation," *Journal of Dynamic Systems Measurement & Control-Transactions of the Asme,* Vol. 115, No. 4, pp. 679-686, Dec 1993.

Rajamani, R., Tan, H.S., Law, B. and Zhang, W.B., "Demonstration of integrated lateral and longitudinal control for the operation of automated vehicles in platoons," *IEEE Transactions on Control Systems Technology,* Vol. 8, No. 4, pp. 695-708, July 2000.

R. Rajamani, C.Zhu and L. Alexander (2003), "Lateral control of a backward driven front-steering vehicle", *Control Engineering Practice*, Vol. 11, No. 5, pp. 531-540, 2003.

Sasipalli, V.S.R., Sasipalli, G.S. and Harada, K., "Single spiral in highway design and bounds for their scaling," *IEICE Transactions on Information and Systems,* Vol. E80-D, No. 11, November 1997.

Taylor, C.J., Kosecka, J., Blasi, R. and Malik, J., "A comparative study of vision-based lateral control strategies for autonomous highway driving," , *International Journal of Robotics Research,* Vol. 18, No. 5, pp. 442-453, May 1999.

Thorpe, C.E., Hebert, M., Kanade, T. and Shafer, S., "Vision and navigation for the Carnegie-Mellon Navlab, " *IEEE Transactions on Pattern Analysis and Machine Intelligence,* Vol. 10, No. 3, pp. 362-373, May 1998.

Wang, D. and Qi, F., "Trajectory planning for a four wheel steering vehicle," *Proceedings of the 2001 IEEE International Conference on Robotics and Automation,* Seoul, Korea, May 21-26, 2001.

http://www.springer.com/978-0-387-26396-0

Vehicle Dynamics and Control
Rajamani, R.
2006, XXVI, 472 p. 196 illus., Hardcover
ISBN: 978-0-387-26396-0